Binary phase diagram of hydrated dimyristoylglycerol-dimyristoylphosphatidylcholine mixtures

Thomas Heimburg,* Ulrich Würz,‡ and Derek Marsh*
Max-Planck-Institut für Biophysikalische Chemie, Abteilungen *Spektroskopie und ‡Kinetik der Phasenbildung, D-3400 Göttingen, Germany

ABSTRACT The thermotropic phase behavior of binary mixtures of dimyristoylphosphatidylcholine with dimyristoyl glycerol (DMPC-DMG) has been studied in aqueous dispersion by using differential scanning calorimetry and spin label electron spin resonance spectroscopy. Phase identifications have been made by means of ^{31}P nuclear magnetic resonance spectroscopy and x-ray diffraction. The binary phase diagram of DMPC-DMG mixtures displays three regions corresponding to the existence of compounds (C1 and C2, respectively) with approximately 1:1 and 1:2 mol/mol DMPC:DMG stoichiometries. The first region displays immiscibility between DMPC and C1 in the low temperature lamellar phase and miscibility of the components in the fluid phase that is lamellar. The second region displays immiscibility between C1 and C2 in the low temperature phase that is lamellar, whereas the fluid phase is of the inverted hexagonal type (H_{II}). The third region displays immiscibility between C2 and DMG in the low temperature phase that is lamellar, whereas the fluid phase is isotropic. The presence of immiscible DMG in the low temperature phase of the third region is indicated by hysteresis in the temperature scans corresponding to conversion between the stable and metastable crystalline polymorphs. Analysis of the first region of the phase diagram using regular solution theory further demonstrates the existence of a DMPC:DMG complex with approximately 1:1 stoichiometry and provides parameters for the nonideality of mixing in the fluid phase.

INTRODUCTION

Diacylglycerols are known to activate the important regulatory enzyme protein kinase C when it is associated with membrane phospholipids (Nishizuka, 1984, 1986). Possible mechanisms of activation may involve either a direct molecular interaction of the diacylglycerol with the protein or the recognition of a particular local surface membrane structure by the enzyme. In either case, the interaction is likely to depend on the way in which the diacylglycerol, which is transiently generated in the membrane via the phosphatidylinositol turnover cycle (Berridge, 1984), is presented at the membrane surface. In the second case, the activation will also depend in detail on the lipid structures that may be created by a high local concentration of the diacylglycerol. Additionally, diacylglycerols that are generated locally during phospholipid hydrolysis by phospholipase C also have been shown to be capable of activating both this enzyme and other phospholipases, most probably by a modification of the lipid structure (Dawson et al., 1983, 1984). It is interesting further to note in this connection that it has been demonstrated recently that quite low concentrations of diacylglycerol are capable of inducing conformational changes in another membrane-bound peripheral protein, namely cytochrome *c* (Heimburg et al., 1991).

A systematic approach to the mixing behavior of diacylglycerols with membrane phospholipids is the determination of the binary phase diagrams (cf. e.g., Cevc and Marsh, 1987). Partial phase diagrams, in the region of low diacylglycerol content, have been published for mixtures of dipalmitoyl phosphatidylcholine with various diacylglycerols (Ortiz et al., 1988). For these composition ranges, the systems are likely to remain wholly lamellar in structure on conversion to the fluid phase (De Boeck and Zidovetzki, 1989). From the point of view of mechanisms for activation of protein kinase C and other membrane-bound enzymes, it is of greater interest to investigate the behavior at higher contents of diacylglycerol, also since the latter are more likely to modify the lipid phase structure. Experiments at higher temperatures in the fluid phase and at higher diacylglycerol contents have revealed nonlamellar phases in phosphatidylcholine-diacylglycerol systems of heterogeneous chain composition (Das and Rand, 1986). In addition, only by investigating the entire phase diagram is it possible to obtain a more complete view of the molecular interactions involved.

In the present work, we have determined the thermotropic phase diagram for hydrated binary mixtures of dimyristoyl phosphatidylcholine (DMPC)[1] with dimyristoyl glycerol (DMG) over the entire composition range by using differential scanning calorimetry and spin label electron spin resonance (ESR) spectroscopy to establish the phase boundaries. Evidence is presented for the existence of two molecular compounds between DMPC and DMG with stoichiometries of approximately 1:1 and 1:2 mol/mol. These compounds also give rise to different nonlamellar lipid structures in the fluid phase, as evidenced by ^{31}P nuclear magnetic resonance (NMR) and x-ray diffraction studies. Additionally, analysis of the re-

[1] *Abbreviations used in this paper:* 5-DGSL, 1-acyl-2-[5-(4,4-dimethyloxazolidine-N-oxyl)]stearoyl-*sn*-glycerol; DMG, 1,2-dimyristoyl-*sn*-glycerol; DMPC, 1,2-dimyristoyl-*sn*-glycerol-3-phosphocholine; DSC, differential scanning calorimetry; EDTA, ethylenediaminetetraacetic acid; ESR, electron spin resonance; NMR, nuclear magnetic resonance; 5-PCSL, 1-acyl-2-[5-(4,4-dimethyloxazolidine-N-oxyl)]-stearoyl-*sn*-glycero-3-phosphocholine; Tris, tris(hydroxymethyl)-aminomethane.

0006-3495/92/11/1369/10 $2.00

gion of the phase diagram between DMPC and the compound of 1:1 stoichiometry in terms of regular solution theory provides evidence that the thermodynamic behavior of the compound is characterized by the formation of a true molecular complex composed of two or more DMPC and DMG molecules.

MATERIALS AND METHODS

Materials

DMPC was obtained from Fluka AG (Buchs, Switzerland). DMG was prepared from DMPC by the action of phospholipase C (*Bacillus cereus;* Boehringer-Mannheim, Mannheim, Germany) in ether:water mixture (1:1 vol/vol) at 0°C and was extracted from the ether phase. Purity was checked by thin-layer chromatography. Spin-labeled phosphatidylcholine(1-acyl-2-[5-(4,4-dimethyloxazolidine-*N*-oxyl)]-stearoyl-*sn*-glycero-3-phosphocholine [5-PCSL]) was prepared as described in Marsh and Watts (1982). Spin-labeled diacylglycerol (1-acyl-2-[5-(4,4-dimethyloxazolidine-*N*-oxyl)]stearoyl-*sn*-glycerol [5-DGSL]) was prepared from 5-PCSL in the same manner as for the unlabeled lipid.

Sample preparation

The required amounts of DMPC and DMG were codissolved in dichloromethane. For ESR experiments, 1 mol% spin label (5-DGSL) was also added at this stage. For differential scanning calorimetry (DSC) measurements, the lipid solution was prepared directly in the sample pan. The organic solvent was evaporated in a nitrogen gas stream, and the samples were then dried under vacuum for ≥3 h. To the dry lipid (13 mg for DSC samples or 1 mg for ESR samples), 30 μl for DSC samples or 100 μl for ESR samples of 0.1 M KCl, 10 mM tris(hydroxymethyl)-aminomethane, 10 mM ethylenediaminetetraacetate (pH 7.0) was added, and the sample was hydrated by vortex mixing and warming to a temperature above that of the phase transition. For ^{31}P NMR spectroscopy, the lipid mixtures contained 10–20 mg of the phospholipid component and were dispersed in ~1 ml of buffer. For x-ray diffraction studies, an aliquot was withdrawn from the samples prepared for NMR and pelleted for introduction into the x-ray capillary.

DSC

DSC measurements were performed with a calorimeter (model DSC-2; Perkin-Elmer Corp., Instrument Div., Norwalk, CT) equipped with an Intracooler 1. The samples were contained in hermetically sealed stainless steel pans. The reference pan contained an equal volume of buffer to that in the sample under study. Scan rates were 1.25° min^{-1}. Transition enthalpies were determined by measuring the area under the excess heat capacity versus temperature curves by paper weighing.

ESR spectroscopy

ESR spectra were recorded on a 9-G Hz spectrometer (E-Line; Varian Associates, Instrument Division, Palo Alto, CA) equipped with nitrogen gas-flow temperature regulation. The pelleted lipid samples were contained in sealed 1 mm ID 100-μl glass capillaries that were accommodated in a standard 4 mm diam quartz ESR tube that contained light silicone oil for thermal stability. Temperature was measured by a fine-wire thermocouple that was positioned in the silicone oil at the top of the microwave cavity. Continuous temperature scans were performed by locking the spectrometer field to the peak maximum in the $m_I = 0$ manifold of the ESR spectrum by feeding the double-modulated output signal from the low frequency (1 kHz) detection channel to the field control circuit of the field-frequency lock unit (cf. Marsh and Watts, 1981). Critical coupling was maintained by servoadjustment of the coupling iris with continuous monitoring of the microwave detector current. Output of the ESR peak height was displayed against the linearized thermocouple output on an x-y recorder.

^{31}P NMR spectroscopy

Proton-dipolar decoupled 109 MHz ^{31}P-NMR spectra were recorded on a spectrometer (model WH-270; Bruker Analytische Messtechnik GmbH, Karlsruhe, Germany) equipped with a 200-W transmitter and operating in the Fourier-transform mode. Free induction decays were collected with phase cycling, using an rf pulse width of 10 μs and a decoupling power of ~20 W. The duty cycle of the gated decoupling was ~0.2% (5-s recycle delay). Samples were contained in closed 10 mm diam NMR tubes.

x-ray diffraction

x-ray diffraction experiments were performed using a Kratky small-angle x-ray scattering apparatus with slit geometry (a fuller description is given in Würz, 1988). Sample capillaries were mounted in a massive copper housing that was thermostatted with a Peltier device. Nickel-filtered copper Kα radiation (λ = 0.154 nm) was obtained from a fine-focus tube, and diffraction intensity was recorded with a linear position-sensitive detector on an extension tube at a distance of 98.35 cm from the sample. Samples were contained in 1-mm-diam, fine-wall, glass capillaries.

RESULTS AND DISCUSSION

DSC

The DSC scans of binary mixtures of DMPC with DMG in aqueous dispersion and with compositions over the entire range from 0 to 100 mol% DMG are given in Figs. 1 and 2. In Fig. 1, the phase boundaries of the gel and fluid regions in the mixtures as defined by the onset and completion of the endothermic changes in the excess heat capacity for the heating scans and the exothermic changes in excess heat capacity for the cooling scans are seen to be in quite good agreement. In the region up to 45 mol% DMG, the calorimetric scans display an increasingly broad region over which the excess heat capacity changes, as the DMG content increases. Most notably, the onset temperature for the change in excess heat capacity remains essentially constant over this composition range, indicating gel phase immiscibility. At ~45 mol% DMG, the character of the DSC scans change abruptly to a single sharp peak, suggestive of the existence of an isothermally melting compound at this composition. The calorimetrically observed peak in excess heat capacity then remains rather sharp for compositions up to 65 mol% DMG.

In Fig. 2, which refers to higher DMG compositions, there is no longer a good correspondence between the heating scans and cooling scans. This hysteresis corresponds to a metastability at high DMG contents, as is illustrated by the appearance of an exothermic peak in the initial heating scans that disappears after heating the samples to 45°C, followed immediately by cooling, before initiating the heating scan. Metastability is well known in *sn*-1,2-diacylglycerols that are capable of existing in two different crystalline forms (Small, 1986; Kodali et al., 1990). The α-form of DMG is metastable, and

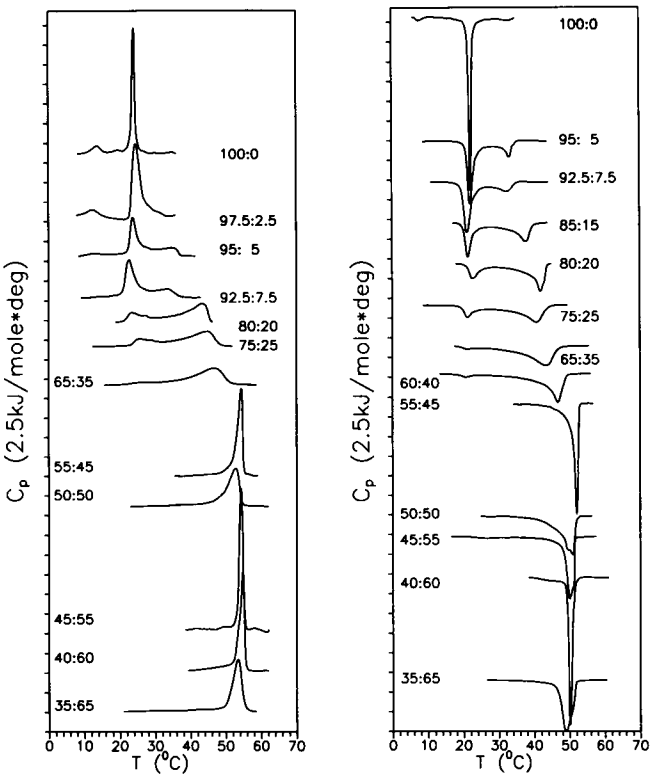

FIGURE 1 DSC scans of binary DMPC-DMG mixtures hydrated in 0.1 M KCl, 10 mM Tris, 10 mM EDTA (pH 7.0) with DMG contents of 0–65 mol%. The DMPC:DMG mole ratios are indicated on the figure. *Left:* heating scans; *right:* cooling scans. Scan rate = 1.25° min^{-1}.

on melting at ~33–35°C transforms exothermically to the stable crystalline β'-form that melts at ~55°C (Fig. 2, *left*). On cooling, hysteresis takes place and the liquid DMG undercools, presumably because the nucleation rate of the β'-phase is very slow compared with the scan rate, until a transition takes place to the metastable α-form at ~33–35°C (Fig. 2, *right*). If a DMG sample is heated to 45°C, cooled to 10°C, and scanned immediately, the metastable transition of the α-form is no longer observed and melting of the β'-form alone takes place at ~55°C (Fig. 2, *middle*). Clearly in this latter case, the stable β'-form is produced from the metastable liquid at 45°C, as indicated by the exothermic transitions that are seen in Fig. 2, *left*.

This metastable behavior of DMG provides considerable help in interpreting the phase behavior of the DMPC-DMG mixtures at high DMG content. The metastable transition characteristic of DMG appears in the DSC scans of samples containing 75 mol% DMG and grows in magnitude with increasing DMG content. This strongly suggests that gel state immiscibility with DMG occurs over this composition range. Because the metastable transition disappears at a DMG content of ~65 mol%, this must correspond to the composition of the immiscible gel phase that coexists with DMG. The temperatures at which the stable and metastable transitions occur also indicate that there is little or no chain migration of the DMG, also in the lipid mixtures. The excess heat capacity changes for the samples that have been preheated to 45°C (Fig. 2, *middle*) have a significant width, indicating that there is a limited range of lateral phase separation for the mixtures at these temperatures.

Binary phase diagram

The phase diagram for the DMPC-DMG mixtures constructed from the temperatures of onset and completion of the excess heat capacity changes in the DSC scans is given in Fig. 3. For DMG contents > 65 mol%, the full lines represent the phase boundaries associated with the stable β' form of DMG (deduced from the scans in the central section of Fig. 2) and the dashed line represents the metastable transition of the α form of DMG. All other boundaries indicated in Fig. 3 represent reversible transitions.

The phase diagram divides itself into three regions that apparently can be associated with compound formation (cf. e.g., Cevc and Marsh, 1987) at DMPC:DMG ratios of ~1:1 and 1:2 mol/mol that are designated by C1 and C2, respectively. Region I corresponds to DMG contents up to ~50 mol% and displays a normal eutectic type of phase diagram in which there is solid phase immiscibility between gel phase DMPC and the compound C1, with the eutectic point lying close to the 0 mol% DMG composition. Region II corresponds to DMG contents between ~50 and 65 mol%. The limits of this region are defined by the point at which the solidus phase boundary of region I at ~20°C disappears and by the point at which the metastable transition of region III at ~35°C disappears. The whole of this region is characterized by a rather narrow transition region that indicates that the transition temperatures of the compounds C1 and C2 are rather similar. Region III corresponds to DMG contents between ~65 and 100 mol%. This region also displays eutectic behavior in which there is solid phase immiscibility between DMG and the compound C2, with the eutectic point lying close to the C2 composition and the region of lateral phase separation being relatively narrow. The latter is consistent with the transition temperature of C2 lying quite close to that of DMG. A characteristic feature of this region is the presence of the metastable transition associated with the α-form of DMG.

The three different regions of the phase diagram are also characterized by different lipid structures in the fluid phase, as is indicated by the designations given in Fig. 3. The ESR spectra of spin-labeled diacylglycerol (cf. below) show that, whereas the fluid phases in regions I and II are of the ordered liquid-crystalline type; that of region III corresponds to an isotropic liquid. The ^{31}P NMR and x-ray diffraction studies (cf. below) further indicate that the liquid-crystalline phase in region I is of the lamellar type but that in region II is of the (inverted) hexagonal type. The phase boundaries between the three

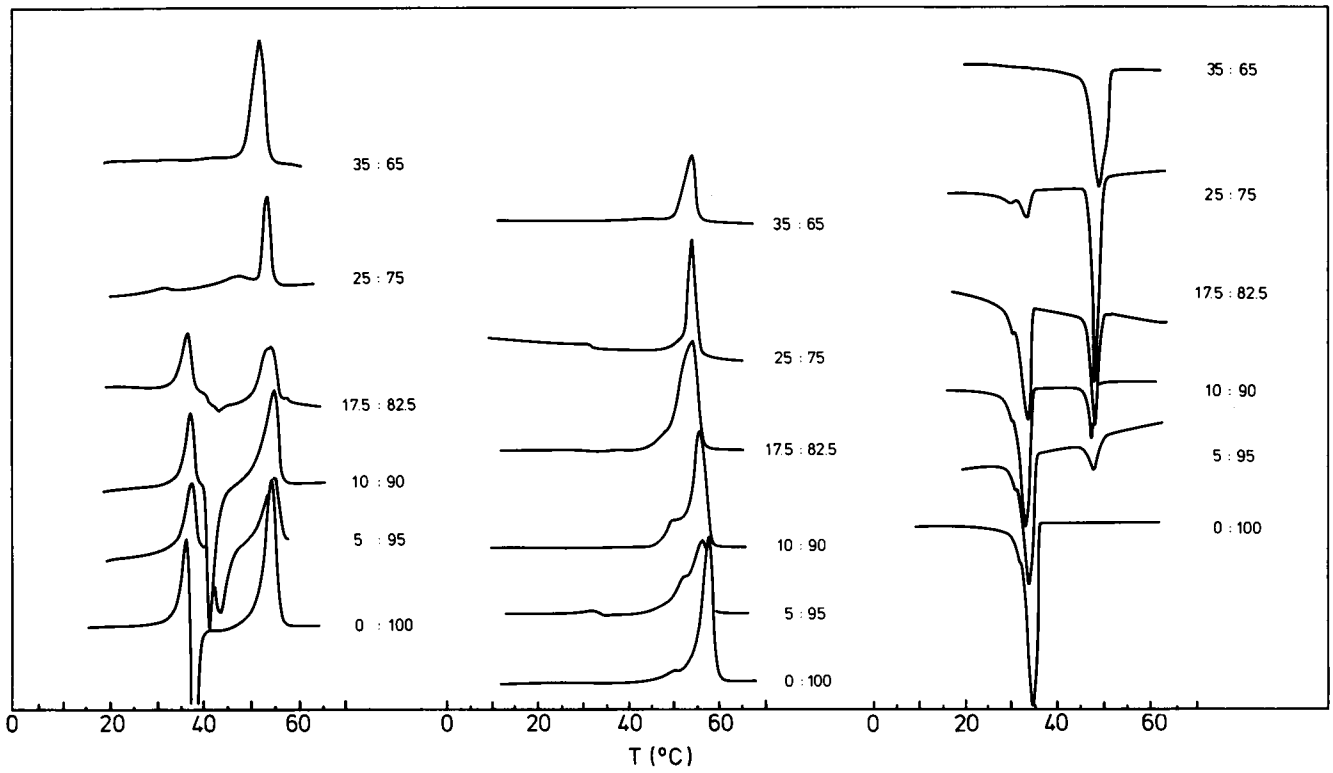

FIGURE 2 DSC scans of binary DMPC-DMG mixtures hydrated in 0.1 M KCl, 10 mM Tris, 10 mM EDTA (pH 7.0) with DMG contents of 65–100 mol%. The DMPC:DMG mole ratios are indicated on the figure. *Left:* heating scans after incubation at 20°C; *middle:* heating scans after heating to 45°C followed directly by cooling to 10°C; *right:* cooling scans. Scan rate = 1.25° min^{-1}.

different fluid phases are indicated solely for simplicity by vertical lines in Fig. 3. They have not been established in detail and, in addition, the existence of intervening phases, e.g., of the cubic type (cf. Heimburg et al., 1990), cannot be excluded. The gel or solid phases of all three regions in the phase diagram are of lamellar structure, as is indicated by both ^{31}P NMR and x-ray diffraction.

ESR

The changes in the lipid dynamics on fluidization during phase separation in the DMPC-DMG mixtures have been studied by spin-label ESR spectroscopy. The results of temperature scans while continuously monitoring the line height of the central peak ($m_I = 0$ manifold) in the ESR spectrum of spin-labeled diacylglycerol, 5-DGSL, in the various mixtures are given in Fig. 4. Increases in spectral line height register increases in extent of rotational motion of the spin-labeled lipid (Marsh and Watts, 1981). The method is preferentially sensitive to the appearance of fluid-phase lipid and hence is particularly appropriate for detecting the boundaries of the region of gel-fluid phase separation. In general, the positions of the phase boundaries detected from the ESR temperature scans are in good agreement with those obtained from the DSC scans (Fig. 3). The transition from the metastable liquid to the stable crystalline β'-form is seen very clearly in the upward temperature scans for the DMG sample. At ~35–36°C, the ESR spectral height returns to that found previously in the solid phase at low temperature. Additionally, the double transition containing the metastable transition of the α-form of DMG is clearly seen for the sample with 80 mol% DMG content in region III. The solidus phase boundary in region I also is reasonably well defined for the sample with 50 mol% DMG content. The calorimetric excess heat capacity is rather low at this point, and therefore the ESR results provide useful confirmation of the occurrence of solid state immiscibility over the entire composition range in region I, as is indicated in the phase diagram of Fig. 3. This is a significant point, since gel phase immiscibility was found only over a much more limited composition range for the corresponding system with palmitoyl chains (Ortiz et al., 1988).

The temperature dependence of the ESR spectra of the 5-DGSL diacylglycerol spin label in a DMPC-DMG mixture of 30 mol% DMG content is shown in Fig. 5, *left*. This sample composition corresponds to region I of the phase diagram, for which the temperature range of lateral phase separation is the largest. The ESR spectra of the gel and fluid phase lipids are distinguished by the different degrees of motional averaging of the spectral anisotropy, as registered by the outer hyperfine splittings that are identified by the dashed lines in Fig. 5. Over the

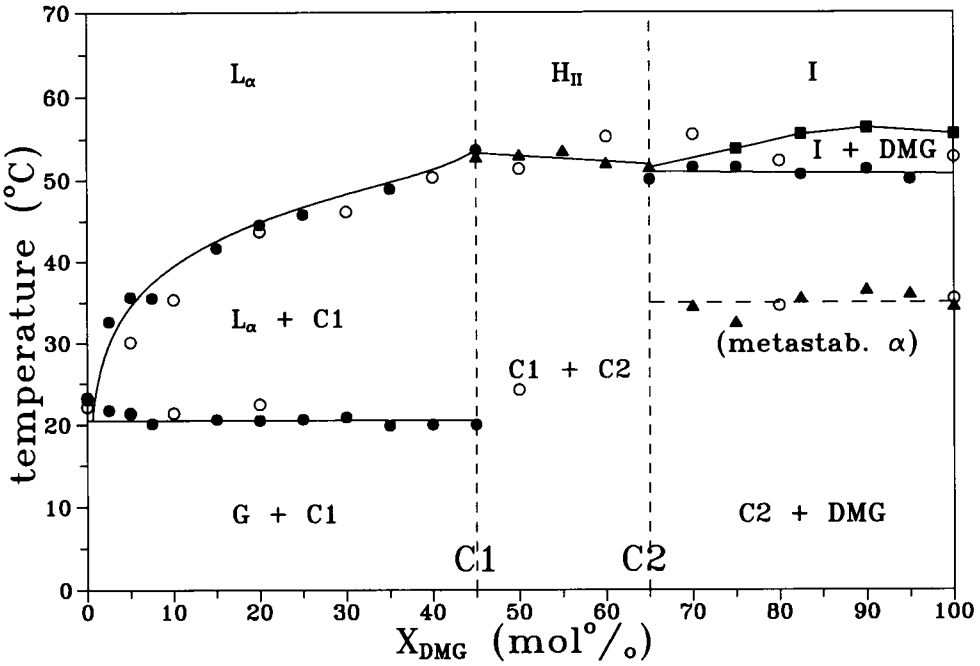

FIGURE 3 Phase diagram for binary DMPC-DMG mixtures hydrated in 0.1 M KCl, 10 mM Tris, 10 mM EDTA (pH 7.0) deduced from the phase boundaries indicated by the DSC scans (*filled symbols*) in Figs. 1 and 2. C1 and C2 denote compounds with DMPC:DMG stoichiometries of approximately 1:1 and 1:2 mol/mol, respectively. DMG represents crystalline dimyristoylglycerol; *G* is the gel phase consisting primarily of DMPC; and L_α, H_{II}, and I are fluid lamellar, inverted hexagonal, and isotropic phases, respectively. "metastab. α" denotes the metastable transition of DMG (α-form). Open circles correspond to phase boundaries deduced from ESR temperature scans.

temperature range between 25 and 35°C, the ESR spectra are composed of two components, one with a large outer hyperfine splitting originating from spin labels in gel phase regions and the other with a smaller outer hyperfine splitting coming from spin labels in fluid phase regions. The observation of the two-component spectra therefore indicates very directly the lateral phase separation that occurs in the two-phase region. The gradual conversion of gel phase regions into fluid phase regions is demonstrated by the systematic change in the relative proportions of the two spectral components over this temperature range.

The temperature dependence of the ESR spectra of the 5-DGSL diacylglycerol spin label in DMG is shown in Fig. 5, *right*. The spectra in the low temperature region have large outer hyperfine splittings characteristic of a rigid phase, but, in contrast to those from the DMPC-DMG mixture from region I, they also display a very marked degree of spin–spin broadening. The latter arises from the limited solubility of the spin-labeled lipid in the crystalline phase of DMG, as opposed to the complete incorporation of the spin label into the gel phase in region I. Also unlike the spectra of the DMPC-DMG mixture from region I, the spectra from 5-DGSL in DMG do not display the coexistence of two components over a wide temperature range. Instead, a transition takes place from a broad single-component spectrum to a narrow single-component spectrum at ~50°C. The spectra from the fluid phase of DMG at temperatures above 50°C are also devoid of spectral anisotropy, demonstrating that the fluid phase of DMG is an isotropic melt and not an ordered liquid crystalline phase as, for instance, in region I for the DMPC-DMG mixture.

^{31}P-NMR

The broad-line proton-dipolar decoupled ^{31}P-NMR spectra of binary mixtures of DMPC with DMG in aqueous dispersion and with compositions over the range from 15 to 82.5 mol% DMG are given in Fig. 6. For samples in the gel phase (Fig. 6, *left*), the spectra are rather similar for all sample compositions and consist of broad, axially anisotropic powder patterns with effective chemical shift anisotropies of $\Delta\sigma \approx -63$ ppm, which are characteristic of phospholipids in a lamellar gel phase.

For samples in the fluid phase (Fig. 6, *right*), the ^{31}P-NMR spectral line shapes change with increasing DMG content. Up to 40 mol% DMG, corresponding to region I of the phase diagram, the spectra consist predominantly of a sharp, axially anisotropic spectrum with chemical shift anisotropy of $\Delta\sigma \approx -45$ ppm, characteristic of a fluid lamellar (L_α) phase. An isotropic peak, which increases with increasing DMG content but is relatively small in terms of the total integrated area, is superimposed on the lamellar powder patterns in this region. The identity of this isotropic peak is not known with certainty; it may correspond to the formation of small particles or to regions of the bilayer surface with a relatively high curvature. In principle, the isotropic peak

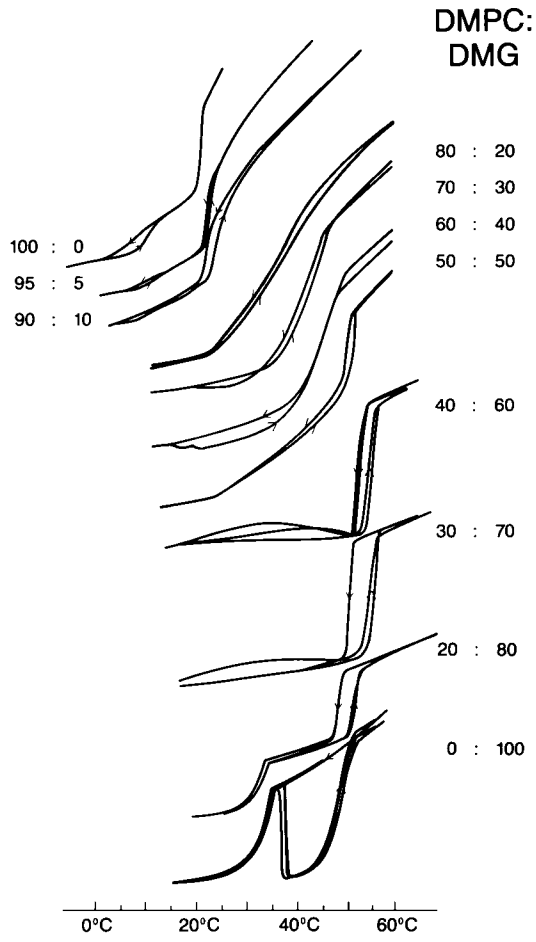

FIGURE 4 Continuous temperature scans of the central line height of the ESR spectrum from spin-labeled diacylglycerol, 5-DGSL, in binary DMPC-DMG mixtures dispersed in 0.1 M KCl, 10 mM Tris, 10 mM EDTA (pH 7.0). The DMPC:DMG mole ratios are indicated on the figure. The direction of the temperature scanning is indicated by the arrows. Scan rate = 1° min^{-1}.

could also correspond to a separate phase, either cubic or an isotropic melt, since this would not be forbidden by the phase rule for a two-component system. If this were the case, the phase boundaries in the fluid region of the phase diagram then would be considerably more complex than those indicated schematically in Fig. 3, possibly including an intermediate (cubic) phase between regions I and II.

For 50 mol% DMG, close to the lower boundary of region II of the phase diagram, the spectrum contains a component characteristic of a phase with cylindrical elements (cf. later) superimposed on a lamellar powder pattern, in addition to a small isotropic peak. It is less likely that the latter corresponds to a separate phase, since three phases can exist only at a unique point in the phase diagram of binary mixtures. At 65 mol% DMG, corresponding essentially to region II of the phase diagram, the spectrum consists predominantly of an axially anisotropic powder pattern with chemical shift anisotropy of $\Delta\sigma \approx +20$ ppm, which is of the opposite sign and approximately one-half the magnitude of that found for the fluid lamellar phase. This spectrum therefore corresponds to a phase with cylindrical symmetry, which from the molecular composition of the system is most probably of the inverted hexagonal (H_{II}) type. The isotropic peak superimposed on this spectrum at 65 mol% DMG most probably corresponds to a coexistence with the isotropic phase found in region III, since at this composition the system is close to the upper boundary of region II. For 74 and 82.5 mol% DMG corresponding to region III of the phase diagram, the spectrum consists solely of a single, isotropic peak. This spectrum is consistent with an isotropic melt, although ^{31}P-NMR is not diagnostic in this respect.

x-ray diffraction

The low angle x-ray diffraction patterns of binary mixtures of DMPC with DMG in aqueous dispersion and with compositions over the range from 0 to 82.5 mol% DMG are given in Fig. 7. The repeat spacings of the various diffraction patterns are given in Table 1. In the gel phase at 15°C, the first two to three orders of a lamellar diffraction pattern are visible at all compositions. A particularly striking feature is that coexisting lamellar patterns, indicative of the gel phase immiscibility, are clearly seen for samples corresponding to regions II and III of the phase diagram. At 82.5 mol% DMG (region III), one component has a much reduced long spacing of 4.3 nm at 15°C and 3.9 nm at 45°C, which is that expected for the α and β' structures, respectively, of pure DMG (see Kodali et al., 1990). Consistent with the phase diagram (Fig. 3), the other component corresponds to the compound C2 with long spacing of 6.3 nm. At 50 mol% DMG, the component with smaller long spacing ($\sim$6.4 nm) corresponds again to the compound C2 and that with the larger long spacing ($\sim$6.6 nm) corresponds to the compound C1. In region I, the repeat spacing of compound C1 is presumably so close to that of the gel G that diffractions from the coexisting immiscible phases are not resolved (cf. Table 1).

In the fluid phase, the first two orders of a lamellar powder pattern are observed for DMPC alone. For the sample with 30 mol% DMG corresponding to region I of the phase diagram, a lamellar diffraction pattern is also observed in the fluid phase, although the second order is rather broad. The latter may be due to a lack of long-range order, which is consistent with the appearance of an isotropic component in the ^{31}P-NMR spectrum. For the sample with 50 mol% DMG, at the lower end of region II, there is a broad diffuse scatter superimposed on which are sharp diffractions whose spacings are in the ratio of $1:\sqrt{3}:2$ (cf. Table 1), characteristic of a hexagonal (H_{II}) phase. For the sample with 82.5 mol% DMG corresponding to region III of the phase diagram, no sharp diffractions are seen. The pattern consists solely of a dif-

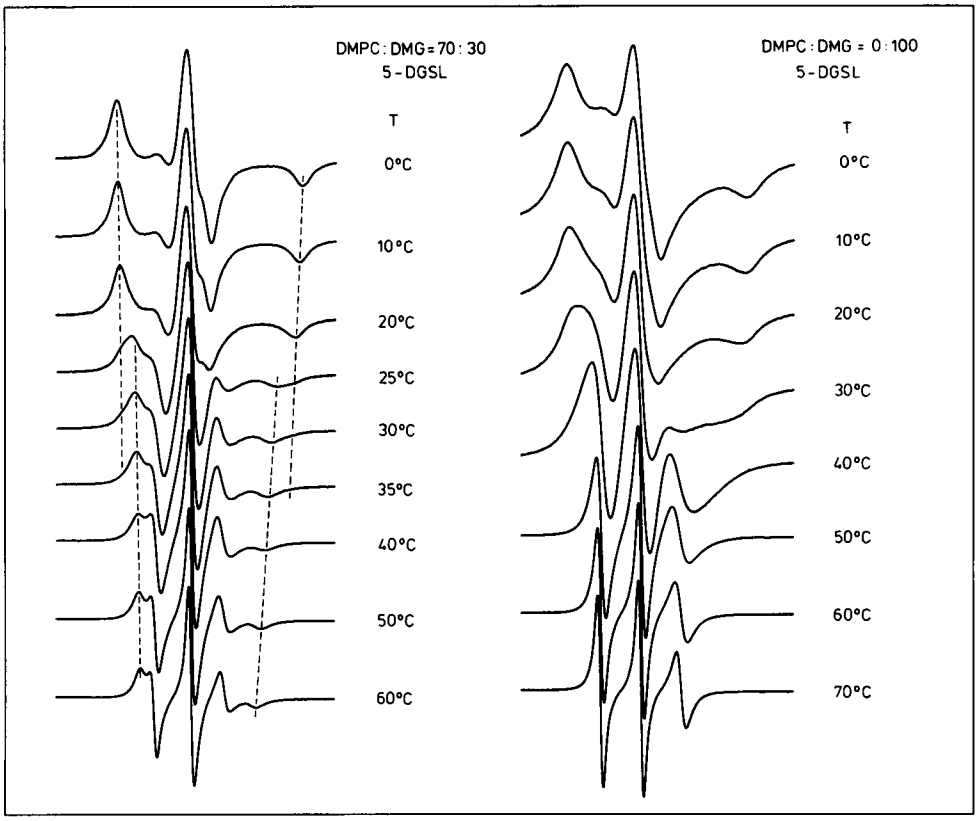

FIGURE 5 Temperature dependence of the ESR spectra from spin-labeled diacylglycerol, 5-DGSL, in a DMPC-DMG (70:30 mol/mol) mixture (*left*) and in DMG (*right*) dispersed in 0.1 M KCl, 10 mM Tris, 10 mM EDTA (pH 7.0). The temperatures at which the spectra were recorded are indicated on the figure. Scan width = 100 G.

fuse scatter that would be consistent with the existence of an isotropic melt, with the DMPC component probably consisting of inverted micelles in this region.

Regular solution theory

The closeness or near identity of the measured solidus and fluidus phase boundaries in regions II and III preclude the possibility of any more detailed analysis of these parts of the phase diagram. However, region I displays a clear eutectic type of behavior that can be substantiated by model calculations and used to obtain further details of the energetics of the molecular interactions. This is done in the following by applying regular solution theory.

The excess free energy arising from nonideal mixing between components A and B is given in regular solution theory by (see e.g., Cevc and Marsh, 1987):

$$\Delta G^{E} = \rho_0 X_A X_B = \rho_0 X_B (1 - X_B) \qquad (1)$$

where X_A and X_B are the mole fractions of components A and B, respectively, and ρ_0 is a measure of the strength of the interaction. For nonideal mixing in both fluid and gel phases, the mole fractions of component B, X_B^S and X_B^F, describing the solidus and fluidus boundaries, respectively, of the phase diagram are given in regular solution theory by the following relations (Cevc and Marsh, 1987):

$$RT \ln (X_B^F/X_B^S) + \rho_0^F (1 - X_B^F)^2 - \rho_0^S (1 - X_B^S)^2 = -\Delta H_B (1 - T/T_B) \qquad (2)$$

and

$$RT \ln [(1 - X_B^F)/(1 - X_B^S)] + \rho_0^F (X_B^F)^2 - \rho_0^S (X_B^S)^2 = -\Delta H_A (1 - T/T_A) \qquad (3)$$

where ρ_0^S and ρ_0^F are the values of ρ_0 for the gel and fluid phases, respectively, and ΔH_A, ΔH_B and T_A, T_B are the transition enthalpies and transition temperatures, respectively, of the pure components A and B. Eqs. 2 and 3 are transcendental in nature and may be solved only numerically by using recursive methods. For certain values of ρ_0, two solutions may be obtained, corresponding, for example, to a phase diagram of the eutectic type.

The Eqs. 2 and 3 have been applied to the eutectic limb of the phase diagram given in Fig. 3 that corresponds to the mixing behavior of DMPC with the compound C1. The stoichiometry of the complex corresponding to C1 has been taken to be generally of the form: $n \cdot$DMPC:$n \cdot$DMG. The molar mass of the C1 complex is therefore:

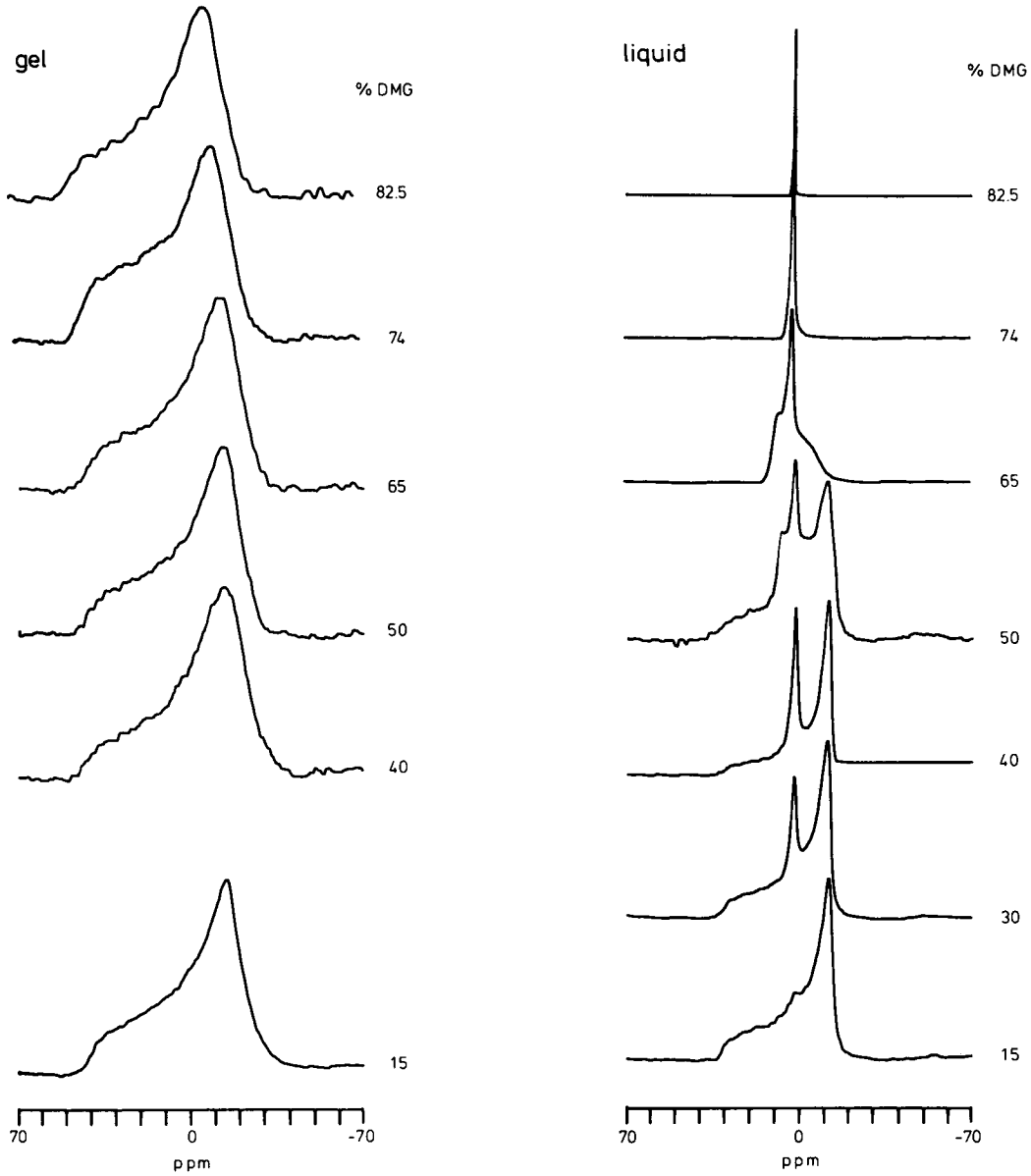

FIGURE 6 Proton-dipolar decoupled 109 MHz ^{31}P-NMR spectra of binary DMPC-DMG mixtures hydrated in 0.1 M KCl, 10 mM Tris, 10 mM EDTA (pH 7.0). The DMPC:DMG mole ratios of the samples are indicated on the figure. *Left:* samples in the gel phase at 25°C, except for 15 and 40 mol% DMG, which are at 15°C; *right:* samples in the fluid phase at 60°C. Chemical shifts (ppm) are referenced to external 85% phosphoric acid.

$$M_{C1} = n(M_{DMPC} + M_{DMG}), \quad (4)$$

where M_{DMPC} and M_{DMG} are the molar masses of DMPC and DMG, respectively. The abscissa in the phase diagram must be expressed in terms of the mole fraction, X_{C1}, of the C1 complex that is therefore given by:

$$X_{C1} = X_{DMG}/[n - (2n - 1)X_{DMG}] \quad (5)$$

which is valid for the region $0 \leq X_{DMG} \leq 0.5$, where X_{DMG} is the mole fraction of DMG in the mixture. The fitting of this section of the phase diagram to the regular solution theory with various values of n is shown in Fig. 8. The measured values of the thermodynamic parameters for DMPC that were used in the fit were $\Delta H_{DMPC} = 26$ kJ · mol^{-1} and $T_{DMPC} = 295.5$ K, and those for the C1 complex were $\Delta H_{C1} = n \times 57$ kJ · mol^{-1} and $T_{C1} = 326$ K. The latter values correspond to those measured for the DMPC-DMG 1:1 mol/mol mixture, where the total transition enthalpy per two-chain lipid is 28.5 kJ · mol^{-1}.

The value of ρ_0^S used for the fit shown in Fig. 8 is simply a lower limit such that gel phase immiscibility is ensured. In contrast, the values of ρ_0^F sensitively determine the shape of the fluidus curve. However, with a value of $n = 1$ for the molecular mass of the C1 complex, no value of ρ_0^F is capable of producing a eutectic point that approaches so closely to the $X_{DMG} = 0$ composition as is observed in the experimental measurements. It

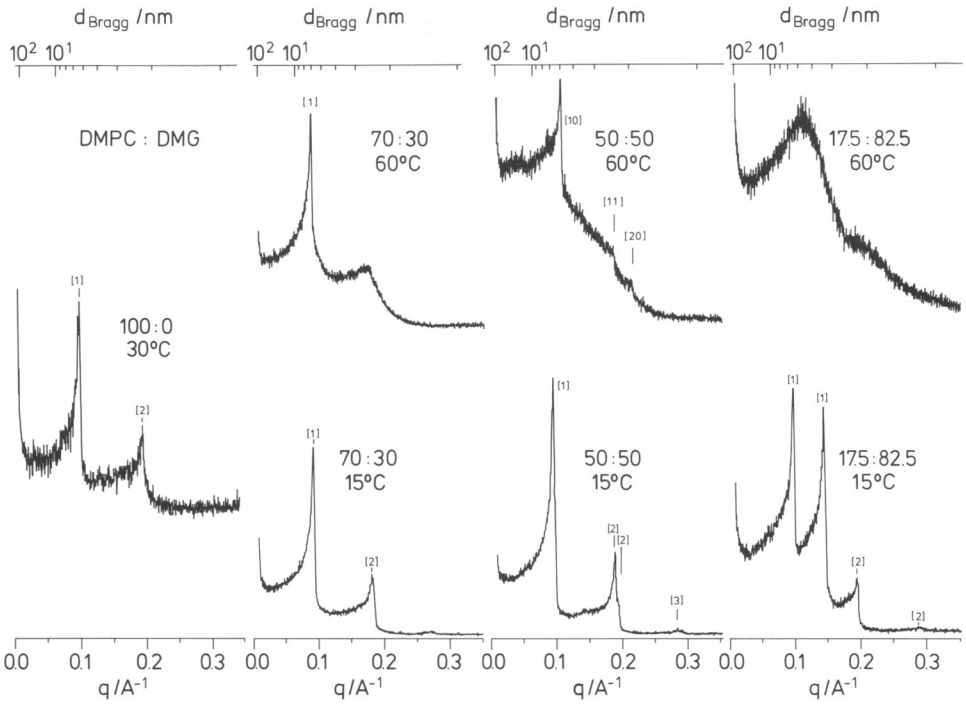

FIGURE 7 Low-angle x-ray diffraction patterns of binary DMPC-DMG mixtures hydrated in 0.1 M KCl, 10 mM Tris, 10 mM EDTA (pH 7.0). The DMPC:DMG mole ratios of the samples and the temperatures at which the diffraction patterns were recorded are indicated on the figure. The indexing of the diffraction orders: [*h*] for lamellar structures and [*hk*] for hexagonal structures, is also indicated on the figure. *Lower:* samples in the gel phase; *upper:* samples in the fluid phase. From left to right: DMPC:DMG = 100:0, 70:30, 50:50, and 17.5:82.5 mol/mol.

must therefore be assumed that the effective molar mass of C1 is greater than that of a simple 1:1 complex. Values of $n \geq 2$ are capable of simulating the observed phase diagram with good accuracy. This increase in effective molecular mass is not in itself sufficient, however, to reproduce the experimental phase diagram; in addition, it is clear that there is nonideality in the mixing of the C1 complexes with DMPC in the fluid phase. It may be noted in passing that several phase diagrams of binary phospholipid mixtures display gel phase immiscibility with the eutectic composition close to that of the pure lower-melting component (see e.g., Marsh, 1990). Therefore, it is quite possible that such effects of a larger apparent molecular mass of the higher-melting component may be operative in these systems also. The experimental solidus phase boundary in Fig. 8 lies slightly below the transition temperature of DMPC (22.5°C), which may be the result of complications arising from the DMPC pretransition that has been ignored in constructing the phase diagram. This may be simulated by taking T_{DMPC} = 20.5°C that, for n = 2, then produces nearly perfect agreement between calculated and experimental phase diagrams and, in fact, corresponds to the solid lines given for region I in Fig. 3.

TABLE 1 Repeat spacings, d_{hk}, in the low angle x-ray diffraction patterns from hydrated DMPC-DMG mixtures

DMPC:DMG	Temperature	*h*, *k*	d_{hk}*
mol/mol	°C		*nm*
100:0	30	1, 0	6.38
		2, 0	3.21
70:30	15	1, 0	6.75
		2, 0	3.40
		3, 0	2.27
	60	1, 0	7.01
50:50	15	1, 0	6.47
		2, 0	3.29, 3.22
		3, 0	2.20, 2.15
	60	1, 0	5.83
		1, 1	3.34
		2, 0	2.90
17.5:82.5	15	1, 0	6.32, 4.33
		2, 0	3.18, 2.14
	45	1, 0	6.34, 3.88
		2, 0	3.21, 2.00
		3, 0	2.14

* Double entries correspond to two independent patterns.

In conclusion, the binary phase diagram of hydrated DMPC-DMG mixtures consists of three distinct eutectic regions that are defined by compound formation at approximate stoichiometries of DMPC:DMG = 1:1 and 1:2 mol/mol. These compounds are characterized by isothermal melting transitions at temperatures close to that for DMG alone. The melting behavior of the 1:1 compound when mixed with DMPC corresponds to a molecular mass that is greater than that for a simple 1:1 complex. This suggests that the 1:1 compound is a defined molecular entity existing in the fluid phase and that it is

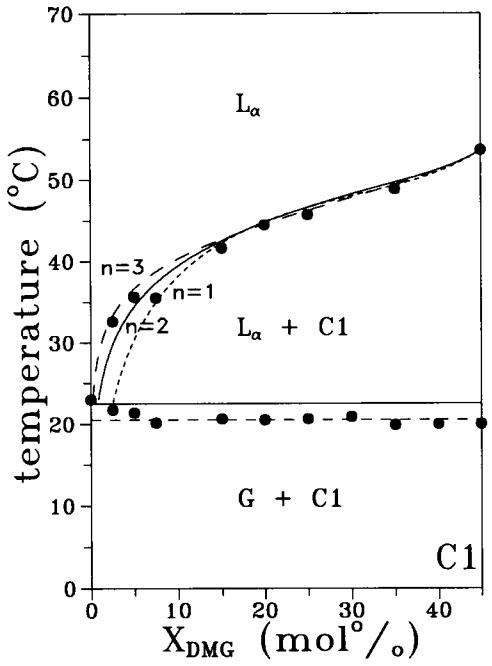

FIGURE 8 Fitting of regular solution theory (Eqs. 2 and 3) to the binary phase diagram for DMPC-DMG mixtures in the region DMPC:DMG = 100:0 to 55:45 mol/mol. The abscissa is scaled according to Eq. 5, with molar masses for the C1 complex given by Eq. 4 with n = 1, 2, and 3. The corresponding transition enthalpies are 26 kJ · mol^{-1} and $n \times 57$ kJ · mol^{-1}, for DMPC and C1, respectively. The interaction energies in the regular solution theory obtained from the fits are ρ_0^S = 22 kJ · mol^{-1} in the gel phase and ρ_0^F = 3.5, 2.4, and 1.2 kJ · mol^{-1} for n = 1, 2, and 3, respectively, in the fluid phase.

stabilized by specific interactions, possibly hydrogen bonding between the DMG —OH group and the ester carbonyls of DMPC. The compound formation correlates with the occurrence of different nonlamellar phases in the fluid regions of the phase diagram, and it is this potential for destabilizing the lamellar membrane structure at high local concentrations of diacylglycerol that may be responsible for the activation of various surface-bound enzymes (cf. e.g., Dawson et al., 1984).

We thank Frau B. Angerstein for her expert technical assistance in synthesizing lipids.

Received for publication 30 January 1992 and in final form 25 June 1992.

REFERENCES

Berridge, M. J. 1984. Inositol triphosphate and diacylglycerol as second messengers. *Biochem. J.* 220:345–360.

Cevc, G., and D. Marsh. 1987. Phospholipid Bilayers. Physical Principles and Models. Wiley-Interscience, New York. 442 pp.

Das, S., and R. P. Rand. 1986. Modification by diacylglycerol of the structure and interaction of various phospholipid bilayer membranes. *Biochemistry.* 25:2882–2889.

Dawson, R. M. C., N. L. Hemington, and R. F. Irvine. 1983. Diacylglycerol potentiates phospholipase attack upon phospholipid bilayers: possible connection with cell stimulation. *Biochem. Biophys. Res. Commun.* 117:196–201.

Dawson, R. M. C., R. F. Irvine, J. Bray, and P. J. Quinn. 1984. Long-chain unsaturated diacylglycerols cause a perturbation in the structure of phospholipid bilayers rendering them susceptible to phospholipase attack. *Biochem. Biophys. Res. Commun.* 125:836–842.

De Boeck, H., and R. Zidovetzki. 1989. Effects of diacylglycerols on the structure of phosphatidylcholine bilayers: a ^{2}H and ^{31}P NMR study. *Biochemistry.* 28:7439–7446.

Heimburg, T., N. J. P. Ryba, U. Würz, and D. Marsh. 1990. Phase transition from a gel to a fluid phase of cubic symmetry in dimyristoylphosphatidylcholine/myristic acid (1:2, mol/mol) bilayers. *Biochim. Biophys. Acta.* 1025:77–81.

Heimburg, T., P. Hildebrandt, and D. Marsh. 1991. Cytochrome *c*-lipid interactions studied by resonance Raman and ^{31}P NMR spectroscopy. Correlation between the conformational changes of the protein and the lipid bilayer. *Biochemistry.* 30:9084–9089.

Kodali, D. R., D. A. Fahey, and D. M. Small. 1990. Structure and polymorphism of saturated monoacid 1,2-diacyl-*sn*-glycerols. *Biochemistry.* 29:10771–10779.

Marsh, D. 1990. CRC Handbook of Lipid Bilayers. CRC Press, Boca Raton, FL. 387 pp.

Marsh, D., and A. Watts. 1981. ESR spin label studies of liposomes. *In* Liposomes: From Physical Structure to Therapeutic Applications. C. G. Knight, editor. Elsevier/North-Holland Biomedical Press, Amsterdam. 139–188.

Marsh, D., and A. Watts. 1982. Spin-labeling and lipid-protein interactions in membranes. *In* Lipid-Protein Interactions. Vol. 2. P. C. Jost and O. H. Griffith, editors. Wiley-Interscience, New York. 53–126.

Nishizuka, Y. 1984. The role of protein kinase C in cell surface signal transduction and tumor promotion. *Nature (Lond.).* 308:693–698.

Nishizuka, Y. 1986. Studies and perspectives of protein kinase C. *Science (Wash. DC).* 233:305–311.

Ortiz, A., J. Villalain, and C. Gomez-Fernandez. 1988. Interaction of diacylglycerols with phosphatidylcholine vesicles as studied by differential scanning calorimetry and fluorescence probe depolarization. *Biochemistry.* 27:9030–9036.

Small, D. M. 1986. The Physical Chemistry of Lipids. Plenum Press, New York and London. 672 pp.

Würz, U. 1988. Small angle x-ray scattering of microemulsions. *Progr. Colloid Polym. Sci.* 76:153–158.